Scalar mass stability bound in a simple Yukawa-theory from renormalisation group equations

A. Jakovác · I. Kaposvári · A. Patkós

Received: date / Accepted: date

Abstract Functional Renormalisation Group equations are constructed for a simple fermion-scalar Yukawa-model with discrete chiral symmetry, including also the effect of a nonzero composite fermion background beyond the conventional scalar condensate. Two approximate versions consistent with the scale dependent equations of motion are solved, taking into account also field renormalisation. The lower bound for the mass of the scalar field is determined requiring the stability of effective potential in the full momentum range, from the cutoff down to vanishing momentum. Close agreement is demonstrated with the results of previous studies done exclusively in presence of scalar condensate. A semiquantitative explanation is provided both for the negligible effect of the wave-function renormalisation and the narrow dispersion in the scalar mass bounds found from different approximation schemes.

 $\textbf{Keywords} \ \ \text{functional renormalization group} \cdot \ \text{Yukawa systems} \cdot \ \text{stability bound} \cdot \ \text{triviality bound} \cdot \ \text{wavefunction renormalization}$

PACS 11.10.Gh · 11.10.Hi

1 Introduction

The experimentally found mass of the Higgs-field is light in the sense that it is very close to the lower edge of the infrared window (for recent theoretical reviews, see [1,2]). This situation resulted in an increased

A. Jakovác

Institute of Physics, Eötvös University

H-1117, Pázmány Péter sétány 1/A, Budapest, Hungary

E-mail: jakovac@caesar.elte.hu

I. Kaposvári

Institute of Physics, Eötvös University

H-1117, Pázmány Péter sétány 1/A, Budapest, Hungary

E-mail: stevenkaposvari@gmail.com

A. Patkós

MTA-ELTE Biological and Statistical Physics Research Group

H-1117, Pázmány Péter sétány 1/A, Budapest, Hungary

E-mail: patkos@galaxy.elte.hu

number of studies investigating the influence of quantum fluctuations on the stability of the Higgs effective potential. For the characterisation of this influence two conceptually different interpretations were put forward. The first is motivated by the setup of Monte Carlo simulations of the ground state of field theories where one finds no signal for any instability in the continuum limit if the theory defined at the scale of the lattice constant (approximately the inverse momentum cutoff) is stable [3,4,5,6]. Along this line of thought one arrives for any fixed value of the scalar mass at a maximal value of the cut-off beyond which no stable bare Lagrangian can exist with a fixed set of operator content (for instance the set of perturbatively renormalisable operators). In the numerical value of this maximal cutoff considerable flexibility is found when a wider set of bare Lagrangians, where irrelevant operators supplement the quartic interaction potential, is allowed [7,8,9].

The alternative interpretation restricts the bare potential energy of the scalar field to the perturbatively renormalisable quartic power. One investigates the renormalisation group equation of the renormalized quartic coupling embedded into the standard model as a function of the renormalisation scale when the cut-off is sent to infinity [10,11,12,13,14]. One encounters negative value for this coupling upon fixing its "measured" value at some infrared scale, when the renormalisation scale goes beyond a certain, maximally allowed value. The order of magnitude of this "critical" value is the same as of the maximal cutoff value emerging from the first approach. The difference of the two estimates arises from the fact that in the beta-function of the quartic coupling the contributions inversely proportional to the cutoff are omitted, while in the first approach usually the exact cut-off dependence of the fluctuations is taken into account.

In this context it represents an important challenge to treat the dynamical transition in theories with multiple minima of the potential energy starting with configurations belonging to the metastable state [15, 16]. The close agreement of the stability (lower) mass bounds obtained with various techniques ranging from perturbation theory, through semianalytic solution of the functional renormalisation group equations to the lattice simulations give considerable mutual support to the credibility of the results. Continuous improvement of the approximation schemes present in all techniques tests the internal consistency of each of them.

The goal of the present paper is to perform a further test of the selfconsistency of the results obtained with the functional renormalisation group (FRG). Earlier approximate computations were restricted to a one-variable effective potential depending on the single invariant built exclusively from the scalar field. This assumption actually contradicts the effective equation of motion which relates at the actual scale the scalar field to some scalar composite formed from the bispinors. The proposed new versions of the renormalisation group equations (RGE's) extend the previous framework, and their effect will be illustrated on the example of the simplest scalar-fermion Yukawa theory [7].

In this paper we consider the evolution of the potential energy depending also on a second variable, the local scalar composite field formed from the fermions. It will be demonstrated that this broader ansatz leads to a definite, though moderate variation in the scalar mass bound at fixed cutoff or in a different projection, in the maximal allowed momentum for any scalar mass value fixed in the infrared. The resulting small effect is not dramatically surprising, since the expectation value of the composite fermion-condensate vanishes in the partial extremal points of the potential with respect the scalar field variable. The size of the variation reflects the importance of the fluctuations near the extremal point.

On the other hand by exploiting the effective equation of motion one is allowed to construct a version of the RGE, where the Yukawa-coupling is kept fixed and it still provides the same quality lower mass bounds like the variants where the initial value of the Yukawa-coupling is also fine-tuned.

The paper is organised as follows. In section 2 the model and the Ansatz for its scale dependent effective action are introduced. The set of RGE's is constructed explicitly in presence of scalar and fermionic

backgrounds in the formulation due to Wetterich [17,18] (see also [19]). The extra contribution reflecting the presence of the fermionic background is clearly identified. In section 3 two different formulations are proposed for the Local Potential Approximation (LPA) of the Wetterich equation and compared to a previous variant [7]. The relevant RGE's in terms of dimensionless quantities are formulated with help of the Appendix. In section 4 the effect of anomalous dimensions of the scalar and the fermi-fields is introduced into the set of RGE's. Section 5 presents the scalar mass estimates emerging from numerically solving the lowest non-trivial power-function ansatz for the potential. Conclusions are summarised in Section 6.

2 The model and its RGE

The scalar-fermion Yukawa model in Euclidean space-time will be treated in the framework of the following effective action Ansatz defining the theory at scale k:

$$\Gamma_k = \int_{\mathcal{T}} \left[Z_{\psi k} \bar{\psi} \gamma_m \partial_m \psi + \frac{1}{2} Z_{\sigma k} (\partial_m \sigma)^2 + h_k I + U_k(\rho) \right], \qquad \rho = \frac{1}{2} \sigma^2, \quad I = \sigma \bar{\psi} \psi. \tag{1}$$

Here the last two terms represent the potential energy density of the model. $U_k(\rho)$ allows a rather general dependence on ρ , but only a Yukawa-type linear dependence is assumed on the other local invariant of the discrete chiral symmetry:

$$\sigma(x) \to -\sigma(x), \qquad \psi(x) \to \gamma_5 \psi(x), \quad \bar{\psi}(x) \to -\bar{\psi}(x)\gamma_5.$$
 (2)

The explicit RGE's are found by evaluating the right hand side of the general form as proposed in [17,18] and projecting it on (1):

$$\partial_t \Gamma_k[\Phi] = \frac{1}{2} \operatorname{Str} \left\{ (\partial_t R_k) \left[\Gamma_k^{(2)} + R_k \right]^{-1} \right\} = \frac{1}{2} \hat{\partial}_t \operatorname{Str} \log \left[\Gamma_k^{(2)} + R_k \right]. \tag{3}$$

This equation expresses the rate of variation of Γ_k as a function of $t = \ln(k/\Lambda)$. $\Gamma_k^{(2)}$ is the second functional derivative matrix of the effective action, and R_k is the infrared regulator restricting the contribution to the functional trace Str onto the neighbourhood of the actual momentum scale k. The symbol $\hat{\partial}_t$ refers to a t-derivative acting exclusively on R_k . Throughout this paper we shall employ the so-called optimised regulator [20].

A non-zero homogeneous condensate at scale k given as $v_k = Z_{\sigma k}^{1/2} \sigma_k = \sqrt{2Z_{\sigma k}\rho_k}$ in the scalar field σ corresponds to the spontaneous symmetry breaking of the discrete γ_5 transformation. By the equation of motion

$$\frac{\delta \Gamma_k}{\delta \sigma} \Big|_{\sigma_k, \psi_k} = h_k(\bar{\psi}\psi)_k + \sigma_k U_k'(\rho_k) = 0 \to h_k I_k + 2\rho_k U_k'(\rho_k) = 0 \tag{4}$$

a general σ_k (or ρ_k) background at scale k implies also the presence of a non-zero value of $(\bar{\psi}\psi)_k$ (or I_k), except in the stationary points of the potential.

The condensate generates mass for the fermi-field: $m_{\psi,k} = h_k \sigma_k$, which itself varies with the scale. The physical value is reached at k = 0, the physical condensate and the physical mass values are computed from the action $\Gamma_{k=0}$, at which the starting $\Gamma_{k=\Lambda}$ will land after running with help of (3) in form (1) from the cutoff Λ to k = 0:

$$v = Z_{\sigma 0}^{1/2} \sigma_0, \qquad m_{\psi} = h_0 \sigma_0, \qquad m_{\sigma}^2 = U_0'(\rho_0) + 2\rho_0 U_0''(\rho_0) \equiv \tilde{U}_k(\rho_0).$$
 (5)

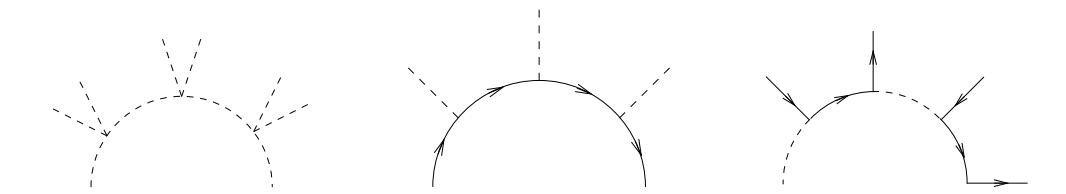


Fig. 1 Propagator sequences building the one-loop contributions to the tracelogs of (7). On the left a piece of a scalar loop (dashed curves) immersed into a scalar condensate, in the middle a fermion loop (continuous curve) immersed into a scalar condensate, on the right a loop constructed of alternating sequence of fermion and scalar propagators immersed into a composite fermionic condensate is represented.

In order to maintain maximal analogy between our model and the top-Higgs sector of the Standard Model, in the discussion of the solution, below we fix the k=0 values of the vacuum condensate to v=246 GeV and the fermion mass to $m_{\psi}=173$ GeV.

A general discussion of the structure of $\Gamma_k^{(2)}$ in presence of the two kinds of background is of order before the detailed expressions based on the ansatz (1) will be explicitly constructed. The second functional derivative of the effective action is represented as a 3x3 matrix:

$$\Gamma_k^{(2)} = \begin{pmatrix}
\Gamma_{\sigma\sigma}^{(2)} & \Gamma_{\sigma\psi}^{(2)} & \Gamma_{\sigma\bar{\psi}^T}^{(2)} \\
\Gamma_{\psi^T\sigma}^{(2)} & \Gamma_{\psi^T\psi}^{(2)} & \Gamma_{\psi^T\bar{\psi}^T}^{(2)} \\
\Gamma_{\bar{\psi}\sigma}^{(2)} & \Gamma_{\bar{\psi}\psi}^{(2)} & \Gamma_{\bar{\psi}\bar{\psi}^T}^{(2)} \\
\Gamma_{\bar{\psi}\sigma}^{(2)} & \Gamma_{\bar{\psi}\psi}^{(2)} & \Gamma_{\bar{\psi}\bar{\psi}^T}^{(2)}
\end{pmatrix},$$
(6)

where the fields are represented by the transposed of the row-vector $(\sigma(x), \psi^T(x), \bar{\psi}(x))$ defining the Gor'kov-Nambu representation of the fermi-field. As a first operation one can transform this matrix into a separate block-diagonal form in the scalar and the fermion-sector [21], which leads for the super-tracelog to

$$\frac{1}{2}\operatorname{Str}\log(\Gamma^{(2)} + R_{k}) = -\frac{1}{2}\operatorname{Tr}\log(\Gamma_{\Psi^{T}\Psi}^{(2)} + R_{k}^{F})
+ \frac{1}{2}\operatorname{Tr}\log(\Gamma_{\sigma\sigma}^{(2)} + R_{k}^{B} - \Gamma_{\sigma\Psi}^{(2)}(\Gamma_{\Psi^{T}\Psi}^{(2)} + R_{k}^{F})^{-1}\Gamma_{\Psi^{T}\sigma}^{(2)})
= -\frac{1}{2}\operatorname{Tr}\log(\Gamma_{\Psi^{T}\Psi}^{(2)} + R_{k}^{F}) + \frac{1}{2}\operatorname{Tr}\log(\Gamma_{\sigma\sigma}^{(2)} + R_{k}^{B})
+ \frac{1}{2}\operatorname{Tr}\log\left[1 - \left(\Gamma_{\sigma\sigma}^{(2)} + R_{k}^{B}\right)^{-1}\Gamma_{\sigma\Psi}^{(2)}\left(\Gamma_{\Psi^{T}\Psi}^{(2)} + R_{k}^{F}\right)^{-1}\Gamma_{\Psi^{T}\sigma}^{(2)}\right].$$
(7)

Here $\Gamma^{(2)}_{\Psi^T\Psi}$ is a compact notation for a hypermatrix in the doubled bispinor field basis and the condensed notation $\Psi^T = (\psi^T, \bar{\psi})$ and its transposed column-vector is used.

Each term has a diagrammatic representation. The first two terms correspond to the free fermion and free boson contributions to the super-tracelog computed in the background σ_k . The last term is the sum of the infinite series of 1-loop contributions containing an increasing number of alternating boson and fermion propagators. At each vertex of fermion-to-boson transformation an external fermion leg joins the loop, due to the assumed presence of a composite fermionic background (see Fig.1).

When one explicitly displays the matrix operations in the bispinor indices in the doubled fermionic sector, one finds for the last term of the previous equation

$$\operatorname{Tr} \log \left[1 - \left(\Gamma_{\sigma\sigma}^{(2)} + R_k^B \right)^{-1} \Gamma_{\sigma\Psi}^{(2)} \left(\Gamma_{\Psi^T\Psi}^{(2)} + R_k^F \right)^{-1} \Gamma_{\Psi^T\sigma}^{(2)} \right]$$

$$= \operatorname{Tr} \log \left[1 - \left(\Gamma_{\sigma\sigma}^{(2)} + R_k^B \right)^{-1} \left[\Gamma_{\sigma\psi}^{(2)} \left(\Gamma_{\bar{\psi}\psi}^{(2)} + R_k^F \right)^{-1} \Gamma_{\bar{\psi}\sigma}^{(2)} \right. \right.$$

$$\left. + \Gamma_{\sigma\bar{\psi}^T}^{(2)} \left(\Gamma_{\psi^T\bar{\psi}^T}^{(2)} + R_k^F \right)^{-1} \Gamma_{\psi^T\sigma}^{(2)} \right] \right]. \tag{8}$$

In earlier papers the super-trace was evaluated on a background exclusively consisting of a nonzero σ -condensate [7]. On such a background $\Gamma_{\sigma\Psi}^{(2)} = \Gamma_{\Psi^T\sigma}^{(2)} = 0$ and the right hand side of the RGE simply reduces to the combination of a pure fermion- and a pure boson-loop. However, this approach for a general choice of the background ρ_k is incompatible with the field equation (4).

In our recent publications clear arguments were put forward [21,22] how the Grassmannian nature of the fermi fields is compatible with a coarse grained background where also nonzero $[(\bar{\psi}\psi)_k]^n$, n>1 terms are present. Earlier this possibility was studied in a series of papers also by Aoki *et al.* [23,24,25, 26].

The entries of the $\Gamma^{(2)}$ matrix are readily found from (1):

$$\Gamma_{\sigma\sigma}^{(2)}(x,y) = (-Z_{\sigma k} \Box + \tilde{U}_{k}(\rho_{k}))\delta(x-y), \qquad \Gamma_{\psi^{T}\psi}^{(2)}(x,y) = \Gamma_{\bar{\psi}\bar{\psi}}^{(2)}(x,y) = 0,
\Gamma_{\sigma\psi}^{(2)}(x,y) = h_{k}\bar{\psi}_{k}(x)\delta(x-y), \qquad \Gamma_{\bar{\psi}\sigma}^{(2)}(x,y) = h_{k}\psi_{k}(x)\delta(x-y),
\Gamma_{\sigma\bar{\psi}^{T}}^{(2)}(x,y) = -h_{k}\psi_{k}^{T}(x)\delta(x-y), \qquad \Gamma_{\psi^{T}\sigma}^{(2)}(x,y) = -h_{k}\bar{\psi}_{k}^{T}(x)\delta(x-y),
\Gamma_{\psi^{T}\bar{\psi}^{T}}^{(2)}(x,y) = (Z_{\psi k}\partial^{T} - h_{k}\sigma_{k}(x))\delta(x-y), \qquad \Gamma_{\bar{\psi}\psi}^{(2)}(x,y) = (Z_{\psi k}\partial + h_{k}\sigma_{k}(x))\delta(x-y). \tag{9}$$

These elements and their inverses will be used in evaluating the three supertraces necessary for the explicit representation of the RGE's of the system.

3 The local potential approximation (LPA)

In this approximation one sets $Z_{\sigma} = Z_{\psi} = 1$ and chooses from the start space-time independent scalar and fermi backgrounds. On this background one has the following representations for the propagators using linear infrared regulators [20]:

$$G_{\psi}(p) = (-iP_F(p)\not p + m_{\psi,k})D_{\psi}(p), \qquad G_{\psi}^T(p) = -(iP_F(p)\not p^T + m_{\psi,k})D_{\psi}(p), \tag{10}$$

and

$$G_{\sigma}^{-1}(p) = P_{B}(p)p^{2} + m_{\sigma,k}^{2}, \quad P_{B} = 1 + r_{B}, \quad r_{B}(p) = \left(\frac{k^{2}}{p^{2}} - 1\right)\Theta\left(\frac{k^{2}}{p^{2}} - 1\right),$$

$$D_{\psi}^{-1}(p) = P_{F}^{2}(p)p^{2} + m_{\psi,k}^{2}, \quad P_{F} = 1 + r_{F}, \quad r_{F}(p) = \left(\frac{k}{\sqrt{p^{2}}} - 1\right)\Theta\left(\frac{k^{2}}{p^{2}} - 1\right). \tag{11}$$

The masses are given with the expressions in (5), but computed with the corresponding fields and couplings defined at scale k.

Below the notation q_R^2 will be used as a short-hand symbol for the momenta appearing in combinations $P_B(q)q^2$ or $P_F^2(q)q^2$, depending on whether one deals with the bosonic or fermionic propagator. One finds with a few algebraic steps the following expression for the rate of evolution of the potential energy density after evaluating $(\bar{\psi}G_{\psi}(q)\psi)_k$ and $(\psi^TG_{\psi}^T(q)\bar{\psi}^T)_k$:

$$\partial_{k}[U_{k}(\rho_{k}) + h_{k}I_{k}] = \frac{1}{2}\hat{\partial}_{k} \int_{q} \left[-4\log(q_{R}^{2} + m_{\psi,k}^{2}) + \log(q_{R}^{2} + m_{\sigma,k}^{2}) + \log\left\{ 1 - h_{k}^{2} \frac{1}{q_{R}^{2} + m_{\sigma,k}^{2}} \frac{2m_{\psi,k}(\bar{\psi}\psi)_{k}}{q_{R}^{2} + m_{\psi,k}^{2}} \right\} \right].$$
(12)

In view of the equality $m_{\psi,k}(\bar{\psi}\psi)_k = h_k I_k$, one recognises that the right hand side is an intrinsically two-variable function of ρ_k and I_k which has to be projected on the ansatz figuring on the left hand side. This expansion is realised by expanding the right hand side around the solution $I_k(\rho_k)$ of the equation of motion (4) and also around the minimum of the effective potential $U_k(\rho_k)$, denoted by $\rho_{k,min}$:

$$RHS(\rho_k, I_k) = RHS(\rho_k, I_k(\rho_{k,min})) + (I_k - I_k(\rho_{k,min})) \frac{\partial}{\partial I_k} RHS(\rho_{k,min}, I_k(\rho_{k,min})) + ...,$$
(13)

where the omitted terms are at least second order in $\rho_k - \rho_{k,min}$ and $I_k - I_k(\rho_{k,min})$. This procedure is analogous to the strategy of [27]. Depending on the order of the expansion one can construct different approximate solutions of the RGE's.

Since there is no unique prescription for this projection, several LPA-variants can be constructed. The theoretical (systematic) error involved in this step can be estimated by the dispersion to be observed in the emerging physical results. Substituting on both sides $I_k = 0$, one recovers the RGE of the potential U_k used in [7], which however is not consistent with (4).

Keeping the first term of (13), one arrives at the following one-variable version of the RGE:

$$\partial_k h_k = 0, (14)$$

$$\partial_k U_k(\rho_k) = \frac{1}{2} \hat{\partial}_k \int_{a} \left\{ -5 \log(q_R^2 + 2h_k^2 \rho_k) + \log\left[(q_R^2 + m_{\sigma,k}^2)(q_R^2 + 2h_k^2 \rho_k) + 4h_k^2 \rho_k U_k'(\rho_k) \right] \right\}. \tag{15}$$

This set of equations differs from the set of LPA-equations discussed in [7] not only by the different rate of evolution of U_k , but also because there a non-trivial running of the Yukawa-coupling was used, derived from the appropriate third functional derivative of the effective action. The present way of projecting (12) on a one-variable LPA will be referred below as *version A*.

A different variant (version B) is arrived at by keeping both terms displayed on the right hand side of (13):

$$\partial_{k}U_{k}(\rho_{k}) = \frac{1}{2}\hat{\partial}_{k} \int_{q} \left\{ -5\log(q_{R}^{2} + 2h_{k}^{2}\rho_{k}) + \log\left[(q_{R}^{2} + m_{\sigma,k}^{2})(q_{R}^{2} + 2h_{k}^{2}\rho_{k}) + 4h_{k}^{2}\rho_{k}U_{k}'(\rho_{k})\right] \right\}$$

$$- \frac{1}{2}\hat{\partial}_{k} \int_{q} \frac{2h_{k}^{3}}{(q_{R}^{2} + m_{\psi,k}^{2})(q_{R}^{2} + m_{\sigma,k}^{2})} \times \frac{2\rho_{k}U_{k}'(\rho_{k})}{h_{k}},$$

$$\partial_{k}(h_{k}I_{k}) = -\frac{1}{2}\hat{\partial}_{k} \int_{q} \frac{2h_{k}^{3}I_{k}}{(q_{R}^{2} + m_{\psi,k}^{2})(q_{R}^{2} + m_{\sigma,k}^{2})} \bigg|_{\rho = \rho_{k,min}}.$$

$$(16)$$

Remarkably the second equation coincides with the RGE of the Yukawa-coupling derived in [7]. This agreement demonstrates the consistency of two different treatments of the Yukawa-coupling. The right hand side of this equation, in view of (13) should be evaluated at $\rho_{k,min}$.

For the solution of the RGE's, they are rewritten in terms of dimensionless (rescaled) fields and couplings as defined in Appendix A. They are distinguished by the lower index 'r'. Also instead of k one introduces as evolution parameter $t = \ln(k/\Lambda)$. The operation $k\hat{\partial}_k$ is performed for the linear regulator of [20] routinely. The equation of u_r in version A has the simple LPA form:

$$\partial_t u_r + du_r + (2 - d)\rho_r u_r' = v_d \left(-\frac{5}{1 + \mu_\psi^2} + \frac{2 + \mu_\psi^2 + \mu_\sigma^2}{(1 + \mu_\psi^2)(1 + \mu_\sigma^2) + 4h_r^2 \rho_r u_r'} \right). \tag{17}$$

(Here the notation $v_d = S_d/(d(2\pi)^d)$, $v_4 = (32\pi^2)^{-1}$ is introduced, with S_d standing for the surface of the d-dimensional unit sphere. For the definition of the rescaled masses μ_{ψ}, μ_{σ} see the Appendix!) The coupled equations of the potential and the Yukawa-coupling for version B are as follows, after cancellation of I_r on both sides of the latter:

$$\partial_t u_r + du_r + (2 - d)\rho_r u_r' = v_d \left(-\frac{5}{1 + \mu_\psi^2} + \frac{2 + \mu_\psi^2 + \mu_\sigma^2}{(1 + \mu_\psi^2)(1 + \mu_\sigma^2) + 4h_r^2 \rho_r u_r'} + 4h_r^2 \rho_r u_r' \frac{2 + \mu_\psi^2 + \mu_\sigma^2}{(1 + \mu_\psi^2)^2 (1 + \mu_\sigma^2)^2} \right).$$
(18)

$$\partial_t h_r^2 + (4 - d)h_r^2 = 4h_r^4 v_d \frac{2 + \mu_\psi^2 + \mu_\sigma^2}{(1 + \mu_\psi^2)^2 (1 + \mu_\sigma^2)^2} \bigg|_{\rho_r = \rho_{r,min}} . \tag{19}$$

The simplest search for the solutions makes use of power series. One finds nontrivial results already with a quadratic expression. In the symmetric phase one has

$$u_r(\rho_r) = \lambda_{1k}\rho_r + \frac{1}{2}\lambda_{2k}\rho_r^2, \qquad \lambda_{1k} > 0, \qquad \mu_\psi^2 = 2h_r^2\rho_r, \qquad \mu_\sigma^2 = \lambda_{1k} + 3\lambda_{2k}\rho_r,$$
 (20)

while the solution in the broken symmetry phase is parametrized as

$$u_r(\Delta \rho = \rho_r - \rho_{r,min}) = \frac{\lambda_{2k}}{2} (\Delta \rho)^2,$$

$$\mu_{\psi}^2 = 2h_r^2 \rho_{r,min} + 2h_r^2 \Delta \rho, \qquad \mu_{\sigma}^2 = 2\lambda_{2k} \rho_{r,min} + 3\lambda_{2k} \Delta \rho,$$
(21)

where $\rho_{r,min}$ is the rescaled minimum of u_r , $(u'_r(\rho_{r,min}) = 0)$. After expanding the right hand side of RGE in power series of ρ_r or $\Delta \rho$ and equating the corresponding terms one arrives at a set of equations for the couplings λ_{nk} and/or the expectation value $\rho_{r,min}$.

The discussion of the influence of the truncation at higher (perturbatively irrelevant) couplings on the stability bound requires some care since truncations at odd powers lead to seemingly unstable potentials with the coefficients in front of the highest power converging to zero from the negative side when $k \to 0$ [28,2]. This fact is seen explicitly already in LPA formulated for the symmetric phase. Assuming that λ_{2k} remains small when one studies the behaviour near the stability edge $\lambda_{2A} = 0$, one finds the following equation for λ_{3k} in case of the RGE variant investigated in [7]:

$$\partial_t \lambda_{3k} = 2\lambda_{3k} + 192v_d h_{rk}^6 + \mathcal{O}(\lambda_{2k}). \tag{22}$$

The right hand side of this equation has a zero with negative fixed point coordinate. It is due to the fermionic loop contribution since the Yukawa-coupling h_r stays very close to its IR (physical) value. Our versions lead to very similar though somewhat more complicated equations. For instance, with version A one finds at $\lambda_2 = 0$

$$\partial_t \lambda_{3k} = 2\lambda_{3k} + 24v_d h_{rk}^2 \left[2h_{rk}^4 \left(5 - \frac{(1+3\lambda_{1k})^2 (3\lambda_{1k}^2 + 6\lambda_{1k} + 1)}{(1+\lambda_{1k})^4} \right) + \lambda_{3k} \frac{2\lambda_{1k}^2 + 6\lambda_{1k} - 1}{(1+\lambda_{1k})^3} \right]. \tag{23}$$

Since λ_{1k} tends to 0 rather quickly when one diminishes t, this equation will behave qualitatively the same way as (22), and this is also true for *version B*. When changing into the broken symmetry phase this fixed point is destabilised and λ_{3k} eventually tends to zero.

This partial fixed point behaviour is an artefact of the power series truncation (for a recent analysis in O(N) models see [29]). The correct asymptotic behaviour of u_r at the fixed point is $\sim \rho_r^{\frac{d}{d-2}}$, as it can be seen from asymptotic analysis of (17). Therefore $u_r = f(\rho_r)\rho_r^{\frac{d}{d-2}}$, where $f(\rho_r) \to 1$ as $\rho_r \to \infty$. As a consequence, the coefficients of the power series expansion of $f(\rho_r)$ have alternating sign. It can be reconstructed with help of the Padé resummation from a sufficiently long power expansion [22]. The infrared values of the physical quantities do not reflect the seemingly unstable behaviour of the odd truncations.

4 Effect of field renormalisations

The two RGE-versions for the potential are modified in the following way, when the anomalous dimensions of the fields are taken into account:

Version A:

$$\partial_t u_k(\rho_r) + du_k(\rho_r) + (2 - d - \eta_\sigma)\rho_r u_k'(\rho_r)$$

$$= v_d \left[-\frac{5}{1 + \mu_\psi^2} \left(1 - \frac{\eta_\psi}{d+1} \right) + \frac{(1 + \mu_\sigma^2) \left(1 - \frac{\eta_\psi}{d+1} \right) + (1 + \mu_\psi^2) \left(1 - \frac{\eta_\sigma}{d+2} \right)}{(1 + \mu_\psi^2) (1 + \mu_\sigma^2) + 4h_r^2 \rho_r u_k'(\rho_r)} \right], \tag{24}$$

Note, that although h_k^2 does not flow in this version, the rescaling of the Yukawa-coupling which takes into account the anomalous dimensions implies for h_r^2 the following running in d=4:

$$h_r^2(t) = h_r^2(t=0)e^{\int_0^t dt(\eta_{\sigma,k} + 2\eta_{\psi,k})}.$$
 (25)

Version B:

$$\partial_{t}u_{k}(\rho_{r}) + du_{k}(\rho_{r}) + (2 - d - \eta_{\sigma})\rho_{r}u'_{k}(\rho_{r})
= v_{d} \left[-\frac{5}{1 + \mu_{\psi}^{2}} \left(1 - \frac{\eta_{\psi}}{d+1} \right) + \frac{(1 + \mu_{\sigma}^{2}) \left(1 - \frac{\eta_{\psi}}{d+1} \right) + (1 + \mu_{\psi}^{2}) \left(1 - \frac{\eta_{\sigma}}{d+2} \right)}{(1 + \mu_{\psi}^{2})(1 + \mu_{\sigma}^{2}) + 4h_{r}^{2}\rho_{r}u'_{k}(\rho_{r})} \right]
+ v_{d} \frac{4h_{r}^{2}\rho_{r}u'_{k}(\rho_{r})}{(1 + \mu_{\psi}^{2})^{2}(1 + \mu_{\sigma}^{2})^{2}} \left[(1 + \mu_{\psi}^{2}) \left(1 - \frac{\eta_{\sigma}}{d+2} \right) + (1 + \mu_{\sigma}^{2}) \left(1 - \frac{\eta_{\psi}}{d+1} \right) \right].$$
(26)

In this latter version also the Yukawa-coupling has a nontrivial scale dependence:

$$\partial_t h_r^2 + (4 - d - \eta_\sigma - 2\eta_\psi) h_r^2 = v_d \frac{4h_r^4}{(1 + \mu_\psi^2)^2 (1 + \mu_\sigma^2)^2} \left[(1 + \mu_\sigma^2) \left(1 - \frac{\eta_\psi}{d+1} \right) + (1 + \mu_\psi^2) \left(1 - \frac{\eta_\sigma}{d+2} \right) \right] \bigg|_{\theta_\sigma = \theta_0 \text{ min}} . \tag{27}$$

The anomalous dimension of the fermi-field is found from the RGE of the effective action with help of the following projection:

$$d_{\gamma} \frac{\delta(0)}{(2\pi)^{d}} \partial_{k} Z_{\psi k} = \frac{d}{dq^{2}} \left\{ -i \not q^{\alpha_{1} \alpha_{2}} \frac{\delta}{\delta \bar{\psi}^{\alpha_{2}}(-q)} \partial_{k} \Gamma_{k} \frac{\delta}{\delta \psi^{\alpha_{1}}(q)} \right\} \bigg|_{q^{2}=0}.$$
(28)

(The quantity d_{γ} stands for the dimension of the fermionic spinor space, and equals to 4 in our actual calculations with Dirac-fermions.) The consistency of the two sides of this equation is ensured by evaluating the right hand side at some specific value of the background fields. The most natural is to choose the background values which correspond to the minimum of the effective potential: $\rho_{k,min}U'_k(\rho_{k,min})=0, (\bar{\psi}\psi)_{k,min}=0.$

One substitutes into the right hand side of this equation for $\partial_k \Gamma_k$ the three terms of the right hand side of (7) one by one. Since neither $\Gamma_{\sigma\sigma}^{(2)}$ nor $\Gamma_{\Psi^T\Psi}^{(2)}$ does not depend on $\bar{\psi}(x)$ or $\psi(x)$, the first two terms do not contribute. The third term can be rewritten after the substitution of constant scalar background (there is no derivation with respect to the scalar field) as

$$\frac{1}{2} \text{Tr} \log[1 - \hat{Q}], \qquad Q(x, y) = h_k^2 G_{\sigma}(x - u) \left(\bar{\psi}(u) G_{\psi}(u - y) \psi(y) + \psi^T G_{\psi}^T(u - y) \bar{\psi}^T(y) \right). \tag{29}$$

Though the fermionic background is space-time dependent, both propagators are translationally invariant because the constant scalar background defines the mass-terms.

The relevant double functional derivative requires the evaluation of the following functional traces:

$$\frac{i}{2} \not q^{\alpha_1 \alpha_2} \frac{\delta}{\delta \bar{\psi}^{\alpha_2}(-q)} \operatorname{Tr} \log[1 - \hat{Q}] \frac{\delta}{\delta \psi^{\alpha_1}(q)} = -\frac{i}{2} \not q^{\alpha_1 \alpha_2} \left\{ \operatorname{Tr} [1 - \hat{Q}]^{-1} \frac{\delta}{\delta \bar{\psi}^{\alpha_2}(-q)} \hat{Q} \frac{\delta}{\delta \bar{\psi}^{\alpha_1}(q)} + \operatorname{Tr} [1 - \hat{Q}]^{-1} \left(\frac{\delta}{\delta \bar{\psi}^{\alpha_2}(-q)} \hat{Q} \right) [1 - \hat{Q}]^{-1} \left(\hat{Q} \frac{\delta}{\delta \bar{\psi}^{\alpha_1}(q)} \right) \right\}. \tag{30}$$

Making use of the explicit expressions of the propagators one finds that the second term of the previous expression contributes exclusively quantities proportional to $(\bar{\psi}\psi)_k$. Therefore it does not contribute to η_{ψ} . The contribution comes solely from the first term of the curly bracket. After performing the derivations and substituting also constant fermionic background (which implies also $Q(x,y) \to Q(p) \sim (\bar{\psi}\psi)_k = 0$) it leads to

$$\partial_t Z_{\psi} = h_k^2 k \hat{\partial}_k \int_p G_{\sigma}(p) \left[P_F(p) D_{\psi}(p) + \frac{2p^2}{d} \frac{\partial}{\partial p^2} \left(P_F(p) D_{\psi}(p) \right) \right]. \tag{31}$$

The scale dependence of the scalar field renormalisation constant arises only from the contributions of the first two terms of (7), since the σ -derivatives of \hat{Q} are proportional to $(\bar{\psi}\psi)_k$ and therefore vanish

in the minimum of the potential energy. The sum of the contribution from the pure scalar and the pure fermi-loop writes as

$$\partial_t Z_{\sigma} = \frac{2\rho_{k,min}}{d} \left(3U_k'' + 2\rho_0 U_k'''\right)^2 k \hat{\partial}_k \int_p p^2 \left(\frac{\partial G_{\sigma}}{\partial p^2}\right)^2 - \frac{2d_{\gamma} h_k^2}{d} k \hat{\partial}_k \int_p p^2 \left[m_{\psi}^2 \left(\frac{\partial D_{\psi}}{\partial p^2}\right)^2 - p^2 \left(\frac{\partial (P_F D_{\psi})}{\partial p^2}\right)^2\right]. \tag{32}$$

The two equations (31) and (32), however, fully coincide with the scale dependence of the wavefunction renormalisation constants as derived in Ref.[7]. For completeness we quote the result using the dimensionless notational convention of the present paper:

$$\eta_{\psi} = 2v_d h_r^2 \frac{1}{(1 + \mu_{\sigma}^2)^2 (1 + \mu_{\psi}^2)} \left(1 - \frac{\eta_{\sigma}}{d+1} \right) \bigg|_{\rho_r = \rho_{r,min}}, \tag{33}$$

$$\eta_{\sigma} = \frac{2v_d}{(1+\mu_{\psi}^2)^2} \left(\left[(3u_r'' + 2\rho_r u_r''')^2 - 8h_r^4 \right] \frac{\rho_r}{(1+\mu_{\psi}^2)^2} - 2h_r^2 \left(1 - \frac{2}{1+\mu_{\psi}^2} \right) \left[\frac{1}{1+\mu_{\psi}^2} + \frac{1}{2} + \frac{1-\eta_{\psi}}{d-2} \right] \right) \Big|_{\rho_r = \rho_{r,min}}.$$
(34)

Since the model is investigated in the broken symmetry phase where both fields are massive and therefore $\mu_{\psi}^2, \mu_{\sigma}^2 \sim k^{-2}$, these equations imply that $\eta_{\psi}, \eta_{\sigma} \to 0$ when $k \to 0$. The anomalous dimensions actually might influence the evolution of u_r and h_r only at intermediate scales. From (33) and (34) one can express the anomalous dimensions algebraically and substituting them into Eq.(24) or Eqs. (26) and (27) one can proceed to the solution of the resulting equations with the same algorithm as applied in LPA.

5 Results for the scalar mass bound

The most detailed solution of the RGE's we have obtained using for the potential the ansatz (20) and (21), quadratic in ρ . At fixed values of $\lambda_{2,\Lambda}$ and Λ the values of $h_r(t=0)$ and $\lambda_{1,\Lambda}$ or $\rho_{r,min}(t=0)$ were tuned until the physical values of v and m_{ψ} were reached at k=0. The typical behaviour of $\rho_{r,min}(t)$ and $h_r(t)$ can be understood on the example of the $\lambda_{2,\Lambda}=10^{-3}$, $\Lambda=10^{7}$ GeV case. In Fig. 2 one has to recognise that h_r runs dominantly in the symmetric phase. The behaviour of h_r changes similarly in both RGE versions: In full analogy with the decoupling phenomena occurring in the evolution of the potential as the scale k passes below the mass of a field the anomalous dimensions drop abruptly to zero, and as a consequence h_r quickly equals to $h_{k=0}$ fixed by the fermion mass.

At the same time one observes that $\rho_{\tau,min}$ stays nearly zero quite deep in the broken phase (for the chosen parameters it changes into this phase around $t \sim -10$), and starts to increase only when h_r approaches very closely its k=0 value $(Z_{\psi,k}, Z_{\sigma,k} \approx 1)$. When (for larger $\lambda_{2,A}$) one starts the solution of the RGE's in the broken symmetry phase, the evolution is increasingly shorter, the prescribed value of $h_{k=0}$ is reached faster, but the characteristic behaviour of the two couplings are the same.

The evolution of $\lambda_{2,k}$ goes parallel with $\lambda_{1,k}$ (or $\rho_{r,min}$) and h_r . Eventually $\lambda_{2,0}$ determines the value of $m_{\sigma}(\lambda_{2,\Lambda},\Lambda)$. Our results are best summarised in the general landscape of the infrared scalar mass

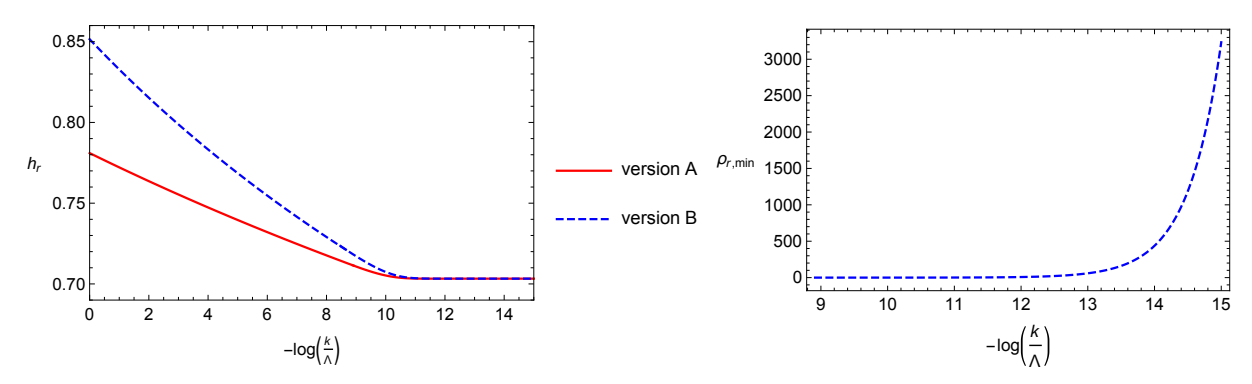


Fig. 2 The running of the Yukawa-coupling in version A and version B and the dimensionless vacuum expectation value (version B) for $\Lambda = 10^7$ GeV and $\lambda_{2,\Lambda} = 10^{-3}$. (In version A $\rho_{r,min}$ follows a very close curve.) The bending of both h_r curves happens when the flow changes from the symmetric into the broken symmetry phase.

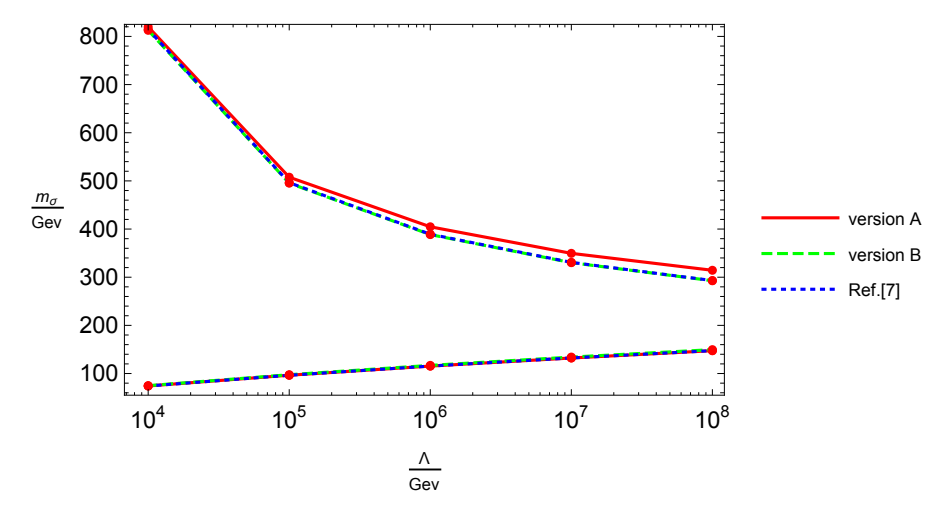


Fig. 3 The cutoff-dependence of m_{σ} for $\lambda_{2,A} = 10^2$ (upper curves) and $\lambda_{2,A} = 10^{-3}$ (lower curves) as obtained in three variants of the RGE's solved at NLO which includes also the running anomalous dimensions of the fields. The continuous line corresponds to *version A*, the dashed one to *version B* of the present paper. The dotted line represents the results of Ref.[7].

values $m_{\sigma}(\lambda_{2,\Lambda}, \Lambda)$ presented in the NLO approximation in Fig. 3 at fixed physical values of the scalar condensate and the fermion mass. In this figure the mass values $m_{\sigma}(\lambda_{2,\Lambda}, \Lambda)$ are displayed only for the smallest $(\lambda_{2,\Lambda} = 10^{-3})$ and the largest $(\lambda_{2,\Lambda} = 10^2)$ values of the "microscopic" quartic coupling. The first set of lines corresponds to the (lower) stability edge of the allowed region, the second (upper) group is very close to the triviality bound. For guiding the eyes straight lines connect the values numerically determined at specific values of the cutoff, and are displayed for each of the three approximate solutions. Together with our versions A and B also the reconstructed values of the approximation scheme of [7] appear. The variation of the mass values among the three projections for any fixed pair $(\lambda_{2,\Lambda}, \Lambda)$ is less than 10%. Lines connecting mass values belonging to some intermediate $\lambda_{2,\Lambda}$ values would arise from a smooth deformation of the lower edge towards the upper one.

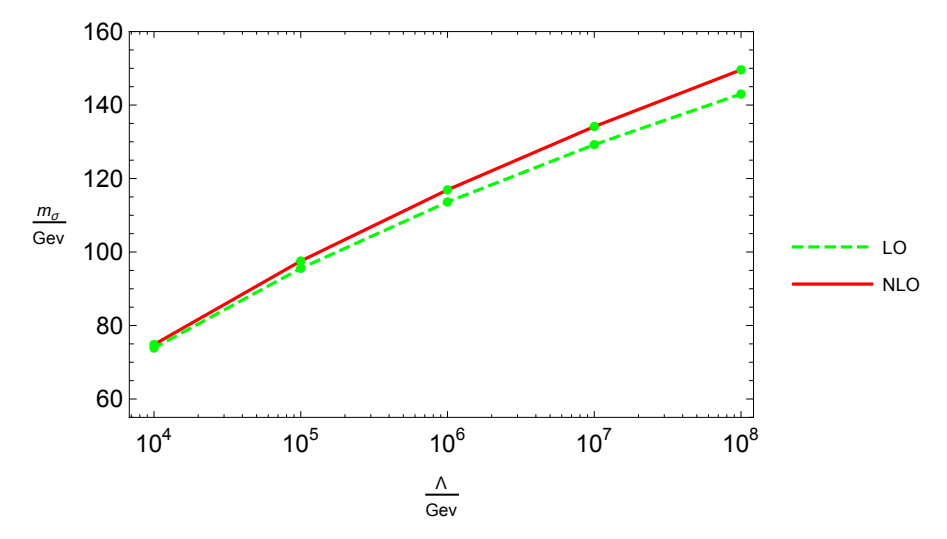
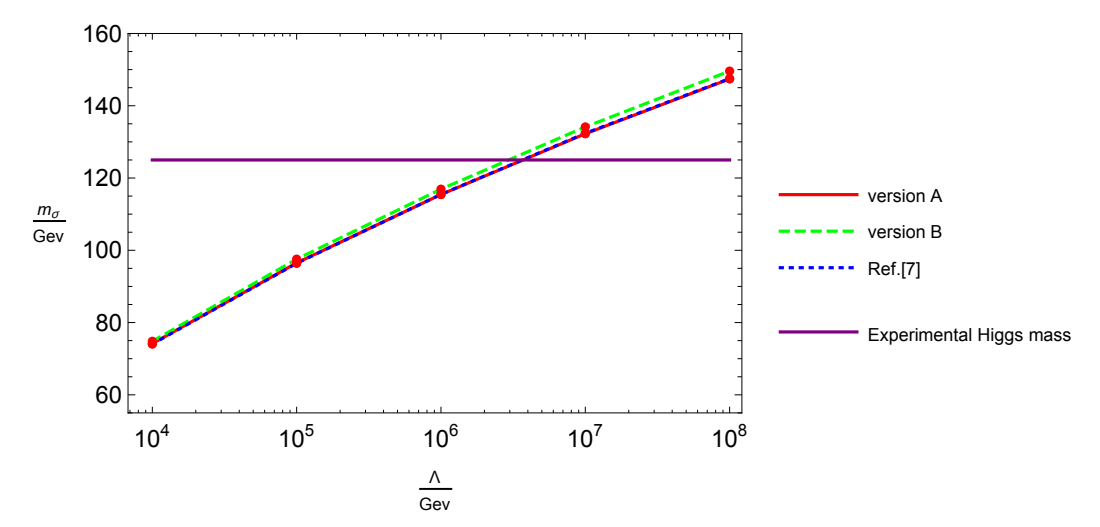


Fig. 4 The effect of taking into account the anomalous dimensions of the fields as compared to the result of the LPA in $version\ B$



 $\textbf{Fig. 5} \ \ \text{The lower mass bounds obtained in the three different projections of the RGE taking into account the anomalous dimensions}$

For the actual empirical situation the location of the (lower) stability edge is more relevant. Here the effect of the wave function renormalisation in $version\ B$ is hardly seen (cf. Fig. 4), and similar situation was observed for $version\ A$ too. The NLO lower bound arising from $version\ A$ remains essentially indistinguishable from the result of [7] as it is obvious from Fig. 5. The curves are slightly shifted to the left (by half order of magnitude), but do not change their profile. A qualitative interpretation of this stability of the NLO results relative to the LO findings is offered making use of the observation made already in [7] and displayed in Fig.2, stating that the effective potential varies slowly in the symmetric phase between the cutoff and the electroweak (physical) scale. It essentially starts to vary around the electroweak scale.

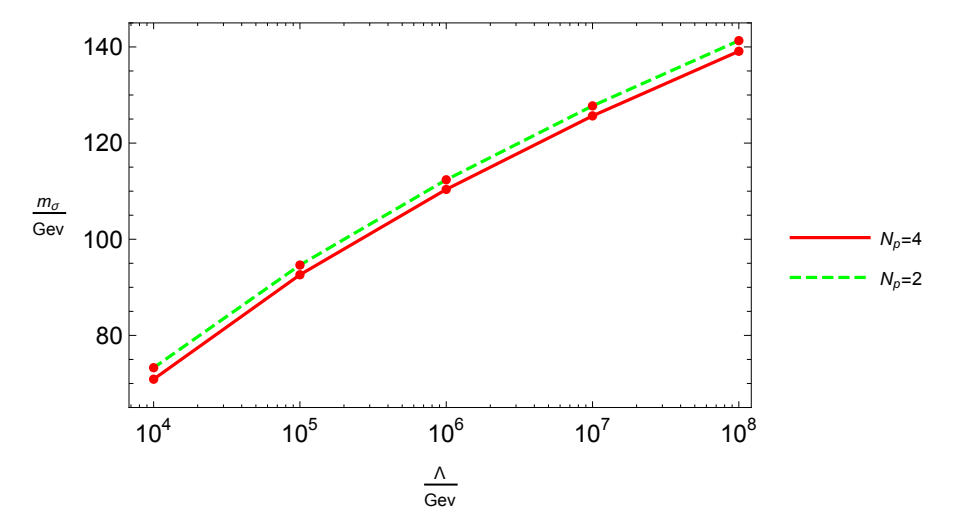


Fig. 6 Comparison of the lower mass bounds obtained using version A of the RGE in the local potential approximation with quadratic and quartic truncations of $u_T(\rho_T)$.

But then there is only a small overlap with the region where the anomalous dimensions differ from zero, therefore there is only a very limited effect of the field renormalisation on the RG-flow. Also the fact that h_r coincides essentially in the region of the evolution of the potential with its k=0 value gives a semiquantitative explanation for the success of version A. One should note that the dispersion of the curves belonging to the three different projections diminishes relative to the LPA.

In view of the lesser number of necessary fine-tunings (one parameter instead of two) the algorithmic simplification present in version A is a nice feature. The finite range of uncertainty of $\Lambda_{max}(m_{\sigma})$ is essentially due to the deviation of version B from version A. The horizontal line in Fig. 5 corresponds to the measured Higgs-mass 125 GeV. When it passes below the curve representing the stability edge, there is no stable "microscopic" theory which could provide the initial conditions for the flow computed by the RGE. The dispersion in the maximal allowed momentum beyond which a non-trivial ultraviolet completion (new physics) is necessary is rather well-defined:

$$2.9 \times 10^6 \text{GeV} < \Lambda_{max}^{(2)} < 3.7 \times 10^6 \text{GeV}.$$
 (35)

The lower bound diminishes about 2-3% when one truncates the power series at higher powers. In Fig.6 the cut-off dependence of the scalar mass is displayed for the LPA in version~A of RGE when also the $\sim \rho_r^4$ term is included into the potential. As an example, we mention that the scalar mass bound changes from 127.74 GeV (quadratic potential) to 125.66 GeV (quartic potential) at $\Lambda=10^7 {\rm GeV}$. The relative change is the same when the wavefunction renormalisation is also incuded and the same observations are made for version~B. These variations shift the range of $\Lambda_{max}^{(4)}$:

$$3.7 \times 10^6 \text{GeV} < \Lambda_{max}^{(4)} < 5.3 \times 10^6 \text{GeV},$$
 (36)

but the change is not significant.

6 Conclusions

In the present paper the lower (stability) edge of the Yukawa theory of a real scalar field with a single Dirac-fermion was investigated carefully based on two new versions of RGE's in the framework of the Functional Renormalisation Group. Relative to previous studies also a composite pointlike fermion background was allowed. The new RGE's represent two alternatives for the consistent use of the equation relating the scale dependent fermionic and scalar backgrounds. The observed RG-flows of the Yukawa coupling and the anomalous dimensions offer a clean interpretation for the stability of the results relative to the one obtained with the simplest variant of LPA involving the tuning of a single parameter at the cutoff.

As our main conclusion we emphasise that the effective potential of the scalar-fermion Yukawa-theory should be treated as a genuine two-variable function of ρ and $\bar{\psi}\psi$. Beyond the dependence of ρ also nonlinear dependence on $\bar{\psi}\psi$ should be investigated in the future by including its higher than linear powers. Only a rather accurate exploration of the "microscopic" structure of the potential will allow the conclusive location of the upper bound on the allowed momenta at a scalar mass fixed in the infrared. At present the truncation of the $\bar{\psi}\psi$ -dependence at rather low powers leads to an unexpectedly well-determined Λ_{max} value, but for assessing the stability of this prediction, operators containing higher powers of the fermionic condensate could be of similar importance like including higher powers of ρ . It is an interesting question if the rather close agreement of all lower mass bounds with the one emerging from the application of a simplified algorithm, where the fermionic condensate is eliminated from the RGE at each step with help of the field equation persists also in higher approximations.

Acknowledgements

The authors thank H. Gies for a helpful correspondence on the effect of polynomial truncations on the stability of the effective potential. This research has been supported by the Hungarian research Fund under the contract No. OTKA-K104292.

Appendix

The dimensionless quantities (bearing the index r) are defined in proportion of the corresponding dimensionful ones defined at scale k, taking into account also their anomalous dimensions, as follows:

$$\rho_{k} = \rho_{r} Z_{\sigma}^{-1} k^{d-2}, \qquad \psi_{k} = \psi_{r} Z_{\psi}^{-1/2} k^{(d-1)/2},
I_{k} = I_{r} Z_{\sigma}^{-1/2} Z_{\psi}^{-1} k^{3d/2-2}, \qquad h_{k} = h_{r} Z_{\sigma}^{1/2} Z_{\psi} k^{2-d/2},
G_{\sigma}(k) = Z_{\sigma}^{-1} k^{-2} g_{\sigma}, \qquad g_{\sigma} = (1 + \mu_{\sigma}^{2})^{-1}, \qquad m_{\sigma}^{2} = Z_{\sigma} k^{2} \mu_{\sigma}^{2},
D_{\psi}(k) = Z_{\psi}^{-2} k^{-2} d_{\psi}, \qquad d_{\psi} = (1 + \mu_{\psi}^{2})^{-1}, \qquad m_{\psi}^{2} = Z_{\psi}^{2} k^{2} \mu_{\psi}^{2}.$$
(37)

The potential $U_k(\rho_k)$ has a canonical dimension but its argument is ρ_r , the dimensionless combination of ρ_k :

$$U_k(\rho_k) = k^d u_k(\rho_r) \big|_{\rho_r = Z_{\sigma k} k^{-d+2} \rho_k}.$$
(38)

Using the above scaling relations one promptly finds

$$\partial_t \rho_r = \rho_k \partial_t (Z_\sigma k^{2-d}) = Z_\sigma k^{2-d} \rho_k (2 - d - \eta_\sigma) = \rho_r (2 - d - \eta_\sigma), \tag{39}$$

with the definition $\partial_t \ln Z_{\sigma} = -\eta_{\sigma}$. From here the t-derivative of the potential follows:

$$\partial_t U_k(\rho_k) = \partial_t (k^d u_k(\rho_r)) = k^d \left[du_k(\rho_r) + \partial_t u_k(\rho_r) + \frac{\partial u_k(\rho_r)}{\partial \rho_r} \partial_t \rho_r \right]$$

$$= k^d (\partial_t u_k(\rho_r) + du_k(\rho_r) + (2 - d - \eta_\sigma) \rho_r u'(\rho_r)). \tag{40}$$

For the t-derivative of the Yukawa-coupling one uses the relation

$$\partial_t(h_k I_k) = \partial_t(k^d h_r I_r) = k^d \left[dh_r I_r + I_r \partial_t h_r + h_r \partial_t I_r \right]$$

$$= k^d I_r \left[\left(d + 2 - \frac{3d}{2} - \frac{1}{2} \eta_\sigma - \eta_\psi \right) h_r + \partial_t h_r \right]. \tag{41}$$

Here one needs also the definition $\eta_{\psi} = -\partial_t \ln Z_{\psi}$. This second equation allows one to cancel I_r from the second equation of (16). An equivalent relation can be directly found for the t-derivative of h_k^2 :

$$\partial_t h_k^2 = Z_{\sigma} Z_{\psi}^2 k^{4-d} \left(\partial_t h_r^2 + (4 - d - \eta_{\sigma} - 2\eta_{\psi}) h_r^2 \right). \tag{42}$$

References

- 1. J.R. Espinosa, PoS LAT2013, arXiv:1311.1970
- 2. A. Eichhorn, H. Gies, J. Jaeckel, T. Plehn, M.M. Scherer, R. Sondenheimer, JHEP 1504, 022 (2015)
- 3. K. Holland and J. Kuti, Nucl. Phys. B Proc. Suppl. 129-130, 765 (2004)
- 4. K. Holland, Nucl. Phys. B Proc. Suppl. 140, 155 (2005)
- 5. Z. Fodor, K. Holland, J. Kuti, D. Nogradi and C. Schroeder, PoS LAT2007, 056 (2007)
- 6. P. Gerhold and K. Jansen, JHEP 0709, 041 (2007) ibid. 0710, 001 (2007), 0907,025 (2009), 1004, 094 (2010)
- 7. H. Gies, C. Gneiting and R. Sondenheimer, Phys. Rev. D89, 045012 (2014)
- 8. H. Gies and R. Sondenheimer, Eur. Phys. J. C75, 68 (2015)
- 9. D.Y.-J. Chu, K. Jansen, B. Knippschild, C.-J. D. Lin and A. Nagy, arXiv:1501.0544
- 10. I.V. Krive and A.D. Linde, Nucl. Phys. B117, 265 (1976)
- 11. A.D. Linde, Phys. Lett. B92, 119 (1982)
- 12. M. Lindner, M. Sher and H.W. Zaglauer, Phys. Lett. B228, 139 (1989)
- 13. G. Degrassi, S. Di Vita, J. Elias-Miro, J.R. Espinosa, G.F. Giudice, G. Isidori and A. Strumia, JHEP 1208, 098 (2012)
- 14. D. Butazzo, G. Degrassi, P.P. Giardino, G.F. Giudice, F. Sala, A. Salvio and A. Strumia, JHEP 1312, 089 (2013)
- 15. B. Bergerhoff, M. Lindner and M. Weiser, Phy. Lett. B469, 61 (1999)
- 16. G. Isidori, G. Ridolfi and A. Strumia, Nucl. Phys. B**609**, 387 (2001)
- 17. C. Wetterich, Nucl. Phys. B**352**, 529 (1991)
- 18. C. Wetterich, Phys. Lett. B**301**, 90 (1993)
- 19. T. Morris, Int. J. Mod. Phys. A9, 2411 (1994)
- 20. D. Litim, Phys. Rev. D64, 105004 (2001)
- 21. A. Jakovác and A. Patkós, Phys. Rev. D88, 065008 (2013)
- 22. A. Jakovác, P. Pósfay and A. Patkós, Eur. Phys. J. C75, 2 (2015)
- 23. K.-I. Aoki, K. Morikawa, J.-I. Sumi, H. Terao and M. Tomoyose, Phys. Rev. D61, 045008 (2000)
- 24. K.-I. Aoki, K. Takagi, H. Terao and M. Tomoyose, Prog. Theor. Phys. 103, 815 (2000)
- 25. K.-I. Aoki and D. Sato, PTEP 2013, 043B04 (2013)
- 26. K.-I. Aoki, S.-I. Kumamoto and D. Sato, PTEP 2014, 043B05 (2014)
- 27. H. Gies and C. Wetterich, Phys. Rev. D65 (2002) 065001
- 28. D.U. Jungnickel and C. Wetterich, Phys. Rev. D53, 5142 (1996)
- 29. P. Mati, Phys. Rev. D 91, 125038 (2015)